

Analysis and Optimization of HARQ for URLLC

Faisal Nadeem, Yonghui Li, Branka Vucetic, Mahyar Shirvanimoghaddam

School of Electrical and Information Engineering, The University of Sydney, NSW, Australia

Emails: {faisal.nadeem, yonghui.li, branka.vucetic, mahyar.shm}@sydney.edu.au

Abstract—In this paper, we investigate the effectiveness of the hybrid automatic repeat request (HARQ) technique in providing high-reliability and low-latency in the finite blocklength (FBL) regime in a single user uplink scenario. We characterize the packet error rate (PER), throughput, and delay performance of chase combining HARQ (CC-HARQ) and incremental redundancy HARQ (IR-HARQ) in AWGN and Rayleigh fading channel with m retransmissions. Furthermore, we consider a quasi-static fading channel model, which is more accurate than the oversimplified i.i.d. block fading or same channel assumption over consecutive packets. We use finite state Markov model under the FBL regime to model correlative fading. Numerical results present interesting insight into the reliability-latency trade-off of HARQ. Furthermore, we formulate an optimization problem to maximize the throughput performance of IR-HARQ by reducing excessive retransmission overhead for a target packet error performance under different SNRs, Doppler frequencies, and rate regimes.

Index Terms—HARQ, Finite blocklength, Rayleigh fading, URLLC.

I. INTRODUCTION

Cellular communications have primarily focused towards increasing spectral efficiency for enhance mobile broadband (eMBB) services. The fifth generation (5G) of mobile standard also includes ultra-reliable low-latency communication (URLLC) and massive machine-type communications (mMTC) into its area of focus [1]. mMTC aims to support internet of things related application; therefore, enabling massive connectivity of devices poses the main challenge [2]. The URLLC is another important direction as it will enable mission-critical services, such as remote surgery and wireless industrial control etc. URLLC is fundamentally challenging as it demands enhancement in two conflicting performance requirements, i.e., low-latency and high-reliability, simultaneously [3]. In particular, for industrial control, a packet of size 32 bytes is required to be delivered with under 1ms latency and packet error rate (PER) of about 10^{-5} , either with or without retransmission [4].

In many communication scenarios, e.g., eMBB, usually packet arrival deadlines are not stringent and the packet size is large. Therefore, repetition of failing packets is a legitimate technique to achieve high throughput [5]. Packet repetition with feedback is very effective in providing resilience against channel deep fades and distortions that arise anytime during transmission and efficient resource utilization [6]. Therefore, in latest communication standards, such as 4G/LTE and 5G, retransmission techniques like the hybrid automatic repeat request (HARQ) are adopted [7]. When a packet is successful with HARQ, the acknowledgment (ACK) signal is fed back

to the transmitter, which sends a new packet; otherwise, it repeats the old packet when a negative ACK (NACK) is received. HARQ has two common types, CC-HARQ and IR-HARQ known as chase combining and incremental redundancy HARQ, respectively. In CC-HARQ, the whole packet is repeated and maximum ratio combining (MRC) is used to increase the reliability. With IR-HARQ, the transmitter sends redundancy by sending a long codeword in chunks and the receiver improves reliability by increasing the decoding performance with a longer codewords after each retransmission. HARQ increases reliability at the expense of increased latency with each retransmission. Therefore, in the latest specifications of 5G, only 1 or 2 retransmissions of HARQ is supported [8]. Both IR-HARQ and CC-HARQ is studies in the finite blocklength (FBL) regime for its effectiveness in URLLC [9, 10].

In addition to the signal-to-noise ratio (SNR) gains, HARQ can also benefit from time diversity of the channel, when its retransmissions experience different channel gains due to relative mobility [6]. In standards communication scenarios, when the packet duration is large, the channel is considered flat during the transmission of a packet and assumed to change independently during its retransmission [5]. Whereas under the FBL regime, the channel is usually considered fixed during the transmission and retransmission of a packet, which is an oversimplification [11]. A more accurate model to characterize the performance of HARQ is the quasi-static fading model [12]. We analyse CC-HARQ and IR-HARQ in both AWGN and Rayleigh fading channel for its effectiveness for URLLC. We characterize the PER, throughput, and delay performance of each HARQ scheme. For the Rayleigh fading channel, we use the finite state Markov channel (FSMC) model to characterize the effect of correlative fading on the HARQ performance. We also optimize the performance of HARQ in different channel conditions, average SNRs, code rates, and Doppler frequencies. Finally, we propose an optimization framework for IR-HARQ to maximize its efficacy in providing the target level of reliability with lower latency.

The rest of the paper is organized as follows. The system model and preliminaries on HARQ in the FBL regime are presented in Section II. In Section III we present reliability, delay analysis, and optimization of HARQ. We provide numerical results in Section IV. Finally, Section V concludes the paper.

II. SYSTEM MODEL AND PRELIMINARIES

We consider a URLLC scenario that a stream of N packets is transmitted and each ℓ -th packet has its arrival deadline T_ℓ .

Let $s(t)$, $y(t)$, and $h(t)$ denote the transmitted signal, received signal, and channel gain at time t , respectively. Then, $y(t)$ is given by:

$$y(t) = h(t)s(t) + w(t), \quad (1)$$

where $w(t) \sim \mathcal{CN}(0, N_0)$ is the circularly symmetric zero-mean complex additive white Gaussian noise (AWGN). We also assume that the total transmit power is $\mathbb{E}[|s(t)|^2] = P_t$ and $s(t)$ is linearly modulated and transmitted with normalized symbol rate 1 symbol/s/Hz. We assume relative mobility between communicating terminals, which causes Doppler fading. The auto correlation function of $h(t)$ is modeled by a zeroth-order Bessel function of the first kind as $J_0(2\pi f_D t)$, where f_D is the Doppler frequency.

A. HARQ in the FBL regime

We enable HARQ retransmissions to recover failing packets. When CC-HARQ is enabled, each failing packet is repeated in the next time slot and MRC is used to combine packets. For IR-HARQ, the transmitter encodes packets using a (n, k) channel code and sends initially $n_1 = \tau_1 n$ symbols. If the packet is not successful (transmitter received a NACK), additional $n_2 = \tau_2 n$ symbols of the codewords are sent. This continues until the transmitter receives an ACK or maximum n symbols are sent.

The packet error rate for CC-HARQ and IR-HARQ with $(m-1)$ retransmissions in the FBL regime can be written as follows [13, 14]¹

$$\epsilon_{cc}([\gamma_i]_1^m) \approx Q\left(\frac{n \log_2(1 + \sum_{i=1}^m \gamma_i) - k + \log_2(n)}{n\sqrt{V(\sum_{i=1}^m \gamma_i)}}\right), \quad (2)$$

$$\epsilon_{ir}([\gamma_i]_1^m, [n_i]_1^m) \approx Q\left(\frac{\sum_{i=1}^m n_i \log_2(1 + \gamma_i) - k + \log_2(\sum_{i=1}^m n_i)}{\sqrt{\sum_{i=1}^m n_i V(\gamma_i)}}\right), \quad (3)$$

where $[x]_1^m = [x_1, \dots, x_m]$, $V(\gamma_i) = (1 - (1 + \gamma_i)^{-2}) \log_2^2(e)$ is the channel dispersion [13], $\gamma_i \in [\Gamma_i]_1^L$ is the SNR at the i -th round of HARQ packet transmission, and $Q(\cdot)$ is the standard Q-function.

B. Time block based FSMC

In order to model correlative fading with finite blocklength of a packet, we consider FSMC. In FSMC, we partition the fading envelop into L fading states using thresholds $\boldsymbol{\eta} = [\eta_0, \eta_2, \dots, \eta_L]$, where $\eta_1 = 0, \eta_{L+1} = \infty$. At any given time, if the channel gain $|h(t)|$ lies in $[\eta_\ell, \eta_{\ell+1}]$, the channel is said to be in state S_ℓ . We set η_ℓ for *equal duration partitioning* of the fading envelop so that n length packet experience single fading state during its transmission [15]. This forms a block by block discrete time channel variation model and form a Markov chain, that is sampled at each time block (TB) shown in Fig.

¹The authors in [12] used a truncated systematic LT code to verify the normal approximation of standard HARQ i.e. (2) and (3).

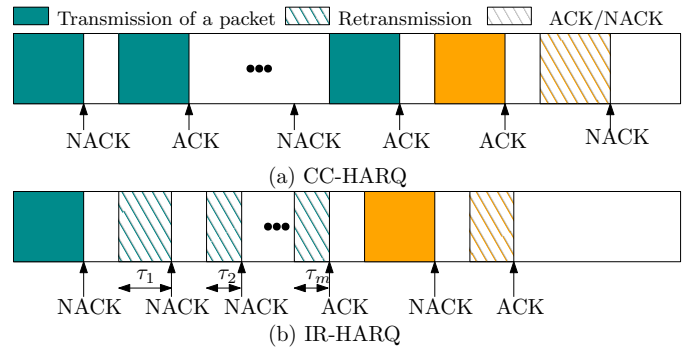


Fig. 1: The packet transmission in IR-HARQ with m retransmissions

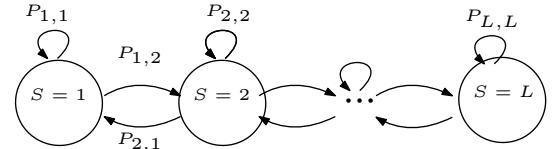


Fig. 2: The transport block based finite state Markov channel (FSMC) model of the Rayleigh fading channel.

2. The fading envelope partition η_ℓ , the TB duration t_{TB} , and the Doppler frequency f_D are sufficient to fully characterize the underlying Markov chain. Under the FBL assumption, we simplify the FSMC by assuming $P_{\ell,k} = 0$ whenever $|\ell - k| > 1$, i.e. a state can only transitions to adjacent states, where $P_{\ell,k}$ is the transition probability from channel fading state ℓ to state k , where $\ell, k \in \mathcal{L}$. This is a valid assumption, because in the FBL regime the channel variation is low across consecutive packets. The state transition probabilities associated with the FSMC model can be calculated as follows [16]:

$$P_{\ell, \ell+1}(\boldsymbol{\eta}, f_D, t_{TB}) \approx \frac{N(\eta_{\ell+1}, f_D) t_{TB}}{q_\ell(\eta_\ell, \eta_{\ell+1})}, \quad 1 \leq \ell \leq L-1, \quad (4a)$$

$$P_{\ell, \ell-1}(\boldsymbol{\eta}, f_D, t_{TB}) \approx \frac{N(\eta_\ell, f_D) t_{TB}}{q_\ell(\eta_\ell, \eta_{\ell+1})}, \quad 2 \leq \ell \leq L \quad (4b)$$

where q_ℓ is the marginal probability of channel being in ℓ -th state given as:

$$q_\ell = \int_{\eta_\ell}^{\eta_{\ell+1}} 2xe^{-x^2} dx, \quad (5)$$

where $f(x) = 2xe^{-x^2}$ is the probability distribution of $|h(t)|$ and under the Bessel auto-correlation function $N(\eta_\ell, f_D)$ is the average number of times per second, the signal envelope $|h(t)|$ crosses level η_ℓ given by [16, 17]:

$$N(\eta_\ell, f_D) = \sqrt{2\pi} \eta_\ell f_D e^{-\eta_\ell^2}. \quad (6)$$

Equation (4) and (6) indicate that state transition probabilities linearly increase with t_{TB} and f_D . Therefore, for total outgoing probabilities of each state to be 1, t_{TB} must be upper bounded as

$$t_{TB} \leq \frac{p_\ell(\eta_\ell, \eta_{\ell+1})}{N(\eta_\ell, f_D) + N(\eta_{\ell+1}, f_D)}, \quad \forall \ell \in \mathcal{L}, \quad (7)$$

where (7) indicates that t_{TB} cannot exceed the average dura-

tion of the state. Following this, we can set the blocklength $n(B, t_{\text{TB}}) = Bt_{\text{TB}}$. Note that thresholds η are uniquely specified to provide equal state duration based on f_{D} and t_{TB} values [15]. With crossover probabilities modeled by AWGN, the symbol level SNR when the channel gain is $|h(t)| = x$, is given by $\gamma(x, t) = \frac{P_t x^2}{BN_0}$. The normalized SNR at the ℓ^{th} channel state, denoted by Γ_ℓ is then given by [12]:

$$\begin{aligned} \Gamma_\ell &= \frac{\int_{\eta_\ell}^{\eta_{\ell+1}} \gamma(x, t) 2x e^{-x^2} dx}{q_\ell(\eta_\ell, \eta_{\ell+1})} \\ &= \frac{P_t}{BN_0} \frac{e^{-\eta_\ell^2}(\eta_\ell^2 + 1) - e^{-\eta_{\ell+1}^2}(\eta_{\ell+1}^2 + 1)}{e^{-\eta_\ell^2} - e^{-\eta_{\ell+1}^2}}. \end{aligned} \quad (8)$$

III. RELIABILITY AND DELAY ANALYSIS

A. AWGN Channel

Let \mathcal{A}_i denote the events that the decoding failed at the receiver after i retransmissions. Then, the probability that a packet is decoded successfully after exactly i retransmissions, denoted as p_i for $i \in \{1, \dots, m\}$, is given by

$$\begin{aligned} p_i &= \text{Prob} \left\{ \mathcal{A}_{i-1} \cap \mathcal{A}_i^c \right\} \\ &= \text{Prob} \{ \mathcal{A}_{i-1} \} - \text{Prob} \left\{ \mathcal{A}_{i-1} \cap \mathcal{A}_i \right\} \\ &\stackrel{(a)}{\approx} \text{Prob} \{ \mathcal{A}_{i-1} \} - \text{Prob} \{ \mathcal{A}_i \} \\ &= \epsilon \left([\gamma]_1^{i-1}, [n_i]_1^{i-1} \right) - \epsilon \left([\gamma]_1^i, [n_i]_1^i \right), \end{aligned} \quad (9)$$

where $n_i = \tau_i n$ and step (a) follows from the fact that the decoding with $i-1$ packet almost certainly fails if the decoding failed with i packets. We also have packet success probability with single transmission as $p_0 = 1 - \epsilon([\gamma_0], [n_0])$, and $p_e = \epsilon([\gamma]_1^m, [n_i]_1^m)$ is the error probability, where $\tau_0 = 1$ and $\epsilon(\cdot)$ is the error rate in the finite blocklength regime which is given in (3) and (2) for IR-HARQ and CC-HARQ, respectively. For CC-HARQ, we have $\tau_i = 1$ as all retransmission packets have the same length as the original packet.

B. Rayleigh fading Channel

In order to characterize the PER of IR-HARQ and CC-HARQ in the Rayleigh fading channel, we assume a finite state Markov channel model (FSMC) [17]. Similar to [12], the FSMC model is used under FBL assumption. In the FSMC, the overall fading envelop is partitioned into L fading states where SNR of ℓ -th fading state denoted as Γ_ℓ . Then the success and fail probabilities of a packet when $m = 2$ can be calculated directly using marginal probabilities of each ℓ -th fading state and transitioning probabilities $P_{\ell,k}$ as follows:

$$p_0 = \sum_{\ell \in \mathcal{L}} q_\ell (1 - \epsilon([\Gamma_\ell], [n_0])) \quad (10)$$

$$p_1 = \sum_{\ell \in \mathcal{L}} \sum_{k \in \mathcal{L}} q_\ell P_{\ell,k} (\epsilon([\Gamma_\ell], [n_0]) - \epsilon([\Gamma_\ell, \Gamma_k], [n_0, n_1])) \quad (11)$$

$$p_e = \sum_{\ell \in \mathcal{L}} \sum_{k \in \mathcal{L}} q_\ell P_{\ell,k} \epsilon([\Gamma_\ell, \Gamma_k], [n_0, n_1]) \quad (12)$$

where q_ℓ is the marginal probability of fading ℓ -th state and $P_{\ell,k}$ is the transition probability between fading state ℓ and k given in detailed in Section II-B.

It is then easy to show that the throughput for HARQ with $m-1$ retransmissions is given by:

$$\eta = \frac{k}{n} \times \frac{1 - p_e}{p_0 + \sum_{i=1}^{m-1} (p_i \sum_{j=0}^i \tau_j) + p_e \sum_{i=0}^{m-1} \tau_i}. \quad (13)$$

The delay distribution for a given packet with HARQ is given by:

$$D[d] = p_0 \delta[d-1] + \sum_{i=1}^{m-1} p_i \delta \left[d - \sum_{j=0}^i \tau_j \right] + p_e \delta \left[d - \sum_{i=0}^{m-1} \tau_i \right] \quad (14)$$

where $\delta[d]$ is the discrete Dirac delta function. It is then easy to show that the overall delay distribution for delivering N packets (either successful or unsuccessful) with HARQ can be found as follows:

$$D_O^{(N)}[d] = \bigotimes_{i=1}^N D[d] \quad (15)$$

where \otimes is the convolution operand. For example, when $m = 2$, the delay distribution of delivering N packets using CC-HARQ is given by [18]:

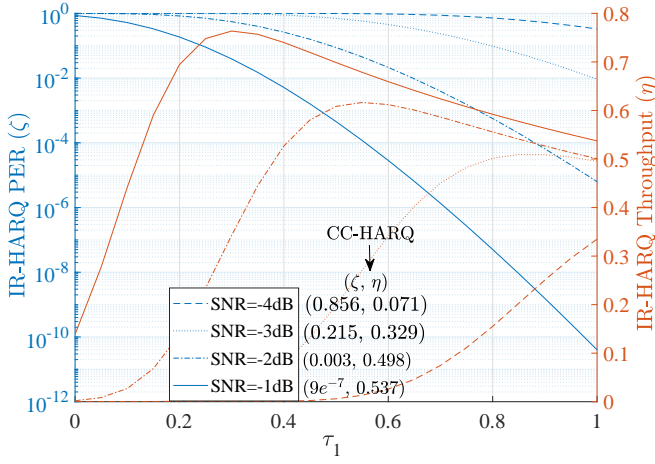
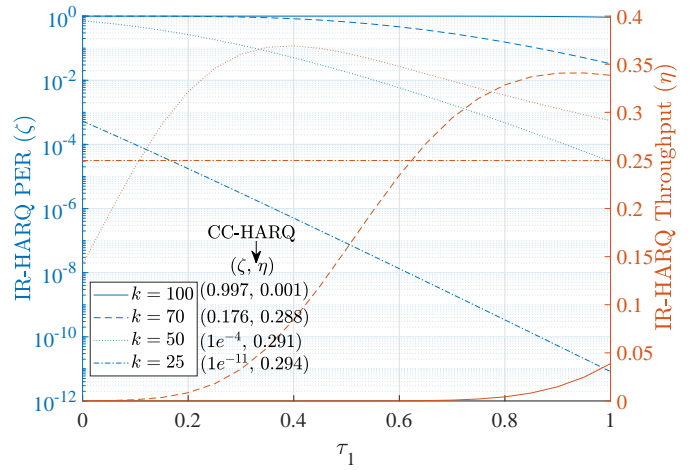
$$\begin{aligned} D_O^{(N)}[d] &= \sum_{i=0}^N \binom{N}{i} (1 - \epsilon([\gamma_0], [n]))^i \epsilon([\gamma_0], [n])^{N-i} \\ &\quad \times \delta[d - (1 + \tau_1)N + i], \end{aligned} \quad (16)$$

IV. NUMERICAL RESULTS

In this section, we present simulation results to highlight the reliability and delay performance of IR-HARQ and CC-HARQ under AWGN and Rayleigh fading channel. The optimization of IR-HARQ is also presented to improve performance further.

A. Performance in AWGN channel

Fig. 3 shows the PER and throughput performance of CC-HARQ and IR-HARQ with different SNRs and rate $R(n, k)$. We vary rate by changing k and keeping n fixed. In CC-HARQ, retransmission is conducted by repeating the entire codeword when requested. For IR-HARQ, PER and throughput versus retransmission coefficient τ_1 is presented. In general, the PER performance of IR-HARQ and CC-HARQ improves by increasing SNRs and reducing rate, i.e. lowering k . The PER improves due to retransmission of failing packet, however, throughput gain starts to saturate for IR-HARQ as the retransmission redundancy increases beyond requirement. For CC-HARQ as the entire codeword is retransmitted; therefore, throughput is not always maximum at a given SNR or k as can be seen in Fig. 3. Because the failing packet sometimes can recover with little redundancy. More specifically, in Fig. 3a for target PER 10^{-4} with IR-HARQ, $\tau_1 = 0.58$ is required at SNR=-1dB in order to achieve highest throughput. When SNR is less, e.g. SNR=-2dB, more retransmission is required to achieve PER 10^{-4} , e.g. $\tau_1 = 1$. On the other hand, with

(a) $k = 100$ 

(b) SNR = -5dB

Fig. 3: Variation of PER and throughput with τ_1 at various SNRs and k for IR-HARQ and CC-HARQ in the AWGN channel when packet length $n = 100$.

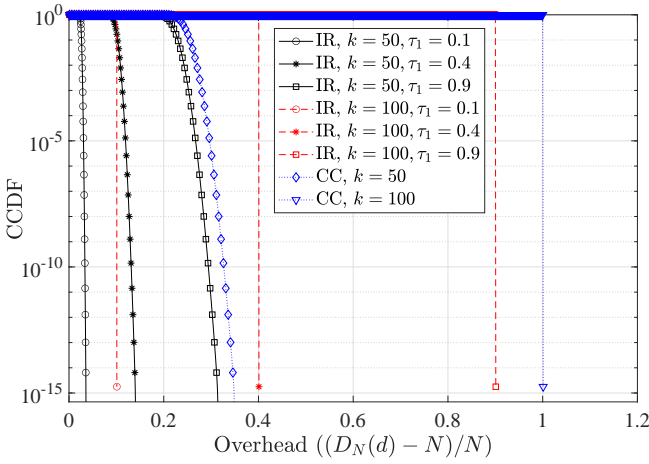


Fig. 4: Delay overhead distribution of CC-HARQ and IR-HARQ at SNR=-4dB and $n = 100$ with different rates R .

CC-HARQ at an SNR=-1dB, the throughput is 0.537 with excessive redundancy.

Fig. 4 shows the delay performance of IR-HARQ and CC-HARQ. We assume that $N = 1000$ packets are scheduled for transmission and each transmission occupies a single time slot. Since retransmissions require additional time slots, we normalize the delay of 1000 packets in Fig. 4. Therefore, when all the packets are delivered with single transmission the delay overhead is zero. Any additional delay due to retransmission is counted as delay overhead. Figure 4 presents the distribution of the delay overhead. As can be seen in Fig. 4, when rate (k) is higher, more packets require retransmission leading to higher delay overhead. Furthermore, each retransmission delays the new arriving packets, leading to queuing and larger delay overheads. A low PER setting, e.g. a small k , reduces the queuing delay; however, this leads to low throughput as shown in Fig 3b. Note that smaller retransmission coefficients τ_1 can significantly limit the queuing delay. Because, a shorter

retransmission reduces the queuing delay of the subsequent packets. Consequently at a target PER and throughput, minimizing τ_1 leads to less queuing delay. For example, at $k = 50$, $\tau_1 = 0.4$ achieves the desired level of reliability with $\approx 20\%$ less packets delay overhead than $\tau_1 = 0.9$.

Fig. 5 shows PER and Throughput performance of IR-HARQ in FBL, when two retransmissions are enabled. For practical consideration, the incremental redundancy increases with each retransmission; therefore, we set $\tau_2 \leq \tau_1$, where τ_2 is the fraction of redundancy in second retransmission. This figure shows that with proper retransmission parameters (τ_1, τ_2), IR-HARQ can achieve a higher reliability. More specifically, with $\tau_1 = \tau_2 = 1$ the maximum redundancy is retransmitted, which corresponds to the lowest PER as can be seen in Fig. 5a. However, Fig. 5b shows that at a fixed SNR, choosing appropriate τ_1 and τ_2 increases throughput with a certain level of PER performance. For example, with $\tau_1 = 0.7$ and $\tau_2 = 0.6$, PER 10^{-4} can be achieved with higher throughput than $\tau_1 = \tau_2 = 1$. Furthermore, with smaller retransmission coefficients, the overall latency and queuing delay is also reduced as can be seen in Fig. 4 for $m = 2$.

B. Performance in Rayleigh fading channel

We utilize FSMC and model the quasi static fading by splitting the fading envelope into L fading states. The boundaries of each fading state are chosen to model equal duration of fading states called equal duration channel partitioning. More specifically, assume c as a channel partitioning parameter representing the number of packets experiencing a specific fading state. The choice of c is usually between 1 and 8 [12]. We set $c = 3.0446$. The channel variability across packets depends upon the length of the packet named as time block duration t_{TB} i.e. $f_D t_{TB}$ value indicates the relative fading speed. In low mobility, i.e. small $f_D t_{TB}$, total number of fading states L needs to be increased for any fixed c to capture the fading variation across consecutive packets more accurately [15]. We study low mobility and high mobility cases with the

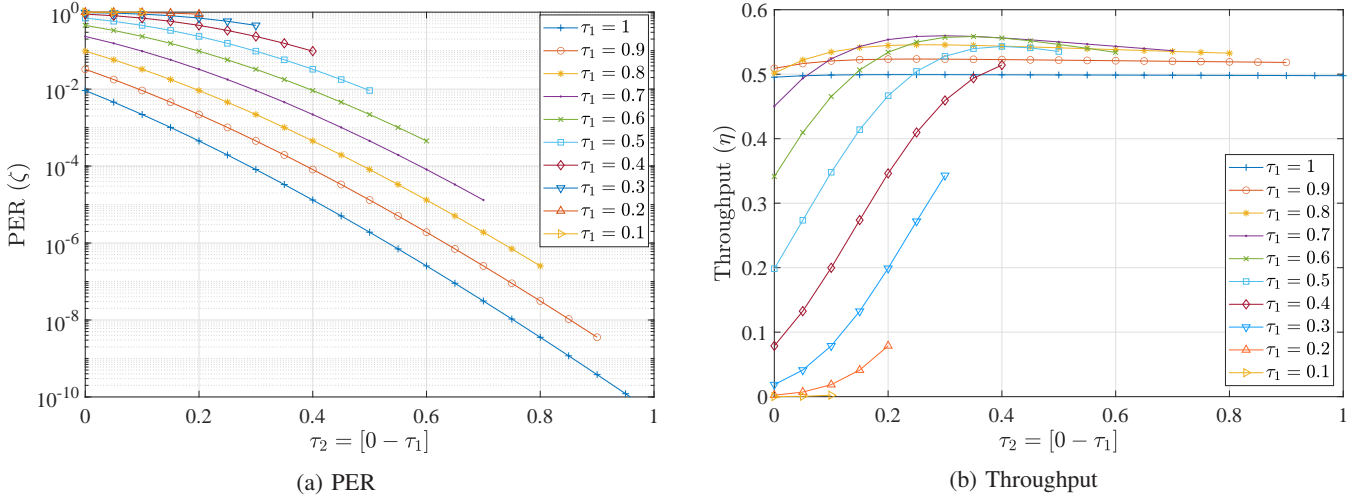


Fig. 5: PER and throughput performance of IR-N-HARQ in the AWGN channel when $m = 3$, $k = 70$, $n = 100$, $\text{SNR} = -4\text{dB}$.

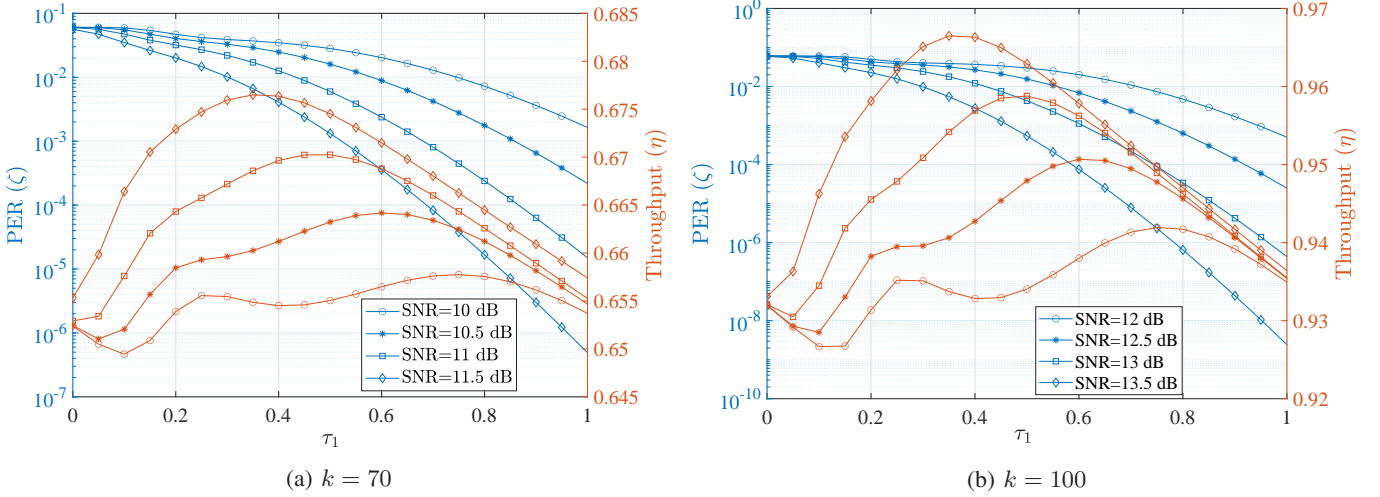


Fig. 6: PER and throughput performance of IR-HARQ with various τ_1 at $n = 100$, $t_{\text{TB}} = 0.00014$ $f_{\text{D}}t_{\text{TB}} = 0.0338$.

following two sets of parameters. When $f_{\text{D}} = 210\text{Hz}$, and $t_{\text{TB}} = 0.14\text{ms}$, we choose $L = 13$ and when $f_{\text{D}} = 285\text{Hz}$, $t_{\text{TB}} = 0.3\text{ms}$ we choose $L = 4$. With carrier frequency $f_{\text{C}} = 1.9\text{GHz}$, these setting capture relative velocity range of 20 – 80 Km/hr.

Fig. 6 shows the PER and throughput performance of IR-HARQ with various τ_1 at different SNRs and information rate R . Similar to AWGN case, overall PER reduces linearly with higher retransmission coefficient in Rayleigh fading case and throughput is saturating due to excessive redundancy. Also, the trend of PER and throughput curves show that there exist trade-off between the achievable PER and throughput. For example in Fig. 6a when $k = 70$, by setting $\tau_1 = 0.4$ the throughput is maximized at 0.675 bits/sec/Hzm when SNR 11.5dB. This parameter setting corresponds to $\text{PER} \sim 10^{-2.5}$. The PER can be further reduced to 10^{-4} by increasing τ to 0.6, which slightly reduces the throughput to 0.625. Fig. 6b shows that increasing information length k and SNRs with proper choice of τ_1 further improves throughput performance.

C. Optimization of retransmission coefficients

With IR-HARQ the retransmission coefficient can be chosen to maximize the throughput for target PER that also results in less queuing delay due to optimal retransmission length. For a given SNR and rate $R(n, k)$, we have the following optimization problem when $m = 2$

$$\begin{aligned} & \max_{\tau_1} \eta & (17) \\ & \text{s.t. } C_1. 0 < \tau_1 \leq 1, \\ & C_2. \zeta \geq \zeta_0, \end{aligned}$$

where C_1 is the range of retransmission coefficient and C_2 implies that the PER should not exceed certain threshold ζ_0 .

Table I presents the optimization of retransmission coefficient τ_1 , when $k = 100$ and 70 with various SNRs to achieve various PER reliability and throughput. The optimized parameters are provided in Table I for the Rayleigh fading case and two different relative mobility scenarios, i.e $f_{\text{D}}t_{\text{TB}} = 0.0338$ and 0.04. Firstly, it can be seen that throughput is maximized

TABLE I: Optimum values of τ_1 for IR-HARQ at $n = 100$ for various SNRs and rate $R(n, k)$.

(a) $k = 100$					(b) $k = 70$				
SNR	$f_D t_{TB} = 0.0338$		$f_D t_{TB} = 0.04$		SNR	$f_D t_{TB} = 0.0338$		$f_D t_{TB} = 0.04$	
	$\hat{\tau}_1$,	(ζ, η)	$\hat{\tau}_1$	(ζ, η)		$\hat{\tau}_1$	(ζ, η)	$\hat{\tau}_1$	(ζ, η)
11	0	0.0605, 0.9319	0.7	0.0055, 0.9330	11	0.5	0.0059, 0.6702	0.2	0.0049, 0.6845
11.5	0.9	0.0089, 0.9323	0.5	0.0093, 0.9440	11.5	0.4	0.0040, 0.6763	0.2	0.0008, 0.6906
12	0.8	0.0047, 0.9417	0.4	0.0064, 0.9546	12	0.3	0.0029, 0.6829	0.1	0.0007, 0.6934
12.5	0.6	0.0068, 0.9506	0.3	0.0047, 0.9652	12.5	0.2	0.0022, 0.6888	0.1	$6.5e^{-5}$, 0.6943
13	0.5	0.0043, 0.9587	0.2	0.0040, 0.9767	13	0.2	0.0003, 0.6925	0.1	$2.7e^{-6}$, 0.6944
13.5	0.4	0.0027, 0.9663	0.2	0.0004, 0.9859	13.5	0.1	0.0002, 0.6940	0.1	$5.0e^{-8}$, 0.6944
14	0.3	0.0019, 0.9745	0.1	0.0004, 0.9908	14	0.1	$1.9e^{-8}$, 0.6944	0.1	$3.6e^{-10}$, 0.6944

by keeping PER at the desired level with τ_1 smaller than 1. Furthermore, as SNR increases, τ_1 can be further reduced while maintaining roughly similar PER and throughput performance. For example, in Table I(a), at $f_D t_{TB} = 0.0338$, ζ 0.0047 and η 0.94 is achieved at SNR 12dB, with $\tau_1 = 0.8$, which reduces to $\tau_1 = 0.6$ with additional 0.5dB SNR for similar reliability. Secondly, when relative mobility increases, τ_1 can be further decreased without losing the PER and throughput performance at a given SNR. More specifically, in Table I(a), similar (ζ, η) performance is achieved with $\tau_1 = 0.4$ when mobility is high i.e. $f_D t_{TB} = 0.04$, whereas when at low mobility, i.e. $f_D t_{TB} = 0.0338$ $\tau_1 = 0.8$. This is primarily due to the fact that with higher relative mobility channel variation between first transmission and its retransmission is higher which provides more diversity and reliability. Therefore, less retransmission is required when mobility is high for a target PER and throughput at fixed SNR or rate. Note that smaller values of τ_1 also leads to less queuing delay as shown in Fig. 4. Table I can be used to select the optimal τ_1 according to fading parameters to avoid excess SNR. For example in I(a), the SNR gain is 0.5dB for target ζ 0.006 and η 0.95. Also as shown in Table I(b), the SNR gap is 2.5 dB at $\tau_1 = 0.1$ for similar PER and throughput target of 10^{-5} and 0.694, respectively.

V. CONCLUSION

In this paper, we analyzed packet retransmission techniques, i.e. IR-HARQ and CC-HARQ, in the FBL regime for URLLC. More specifically, PER, throughput and delay performance is characterized analytically under AWGN and Rayleigh fading channel allowing m retransmissions. Finite state Markov channel model is used to represent quasi-static fading under short packet communication for accurate representation of diversity gain with retransmission. Simulations are carried out to get further insight into the reliability and delay performance of HARQ schemes. Finally, we formulated an optimization problem to maximize throughput for target PER performance under various SNRs and Doppler frequencies. The optimization of retransmission coefficient also translated to the queuing delay minimization.

REFERENCES

[1] H. Holma, A. Toskala, and T. Nakamura, *5G Technology: 3GPP New Radio*. Wiley, 2020.

[2] M. Shirvanimoghaddam, M. Condoluci, M. Dohler, and S. J. Johnson, "On the fundamental limits of random non-orthogonal multiple access in cellular massive IoT," *IEEE Journal on Selected Areas in Communications*, vol. 35, no. 10, pp. 2238–2252, 2017.

[3] H. Chen, R. Abbas, P. Cheng, M. Shirvanimoghaddam, W. Hardjawana, W. Bao, Y. Li, and B. Vucetic, "Ultra-reliable low latency cellular networks: Use cases, challenges and approaches," *IEEE Communications Magazine*, vol. 56, no. 12, pp. 119–125, 2018.

[4] "3GPP TS 22.261 Service requirements for the 5G systems; Stage 1 (Release 17)," 3rd Generation Partnership Project, Technical Specification Group Services and System Aspects, Tech. Rep., Sep. 2020.

[5] T. Shafique, M. Zia, H.-D. Han, and H. Mahmood, "Cross-layer chase combining with selective retransmission, analysis, and throughput optimization for ofdm systems," *IEEE Transactions on Communications*, vol. 64, no. 6, pp. 2311–2325, 2016.

[6] Z. Shi, H. Ding, S. Ma, and K.-W. Tam, "Analysis of HARQ-IR over time-correlated rayleigh fading channels," *IEEE Transactions on Wireless Communications*, vol. 14, no. 12, pp. 7096–7109, 2015.

[7] J. Yang, A. Liu, K. Elmishad, A. Rawat, M. Li, and V. Rawat, "Dynamic HARQ optimization for voice over LTE," in *2018 IEEE International Conference on Communications (ICC)*. IEEE, 2018, pp. 1–5.

[8] "3GPP TR 38.824 Study on physical layer enhancements for NR ultra-reliable low latency communication (URLLC) (Release 16)," 3rd Generation Partnership Project, Technical Specification Group Radio Access Network, Tech. Rep., Oct. 2018.

[9] F. Nadeem, M. Shirvanimoghaddam, Y. Li, and B. Vucetic, "Delay-sensitive noma-harq for short packet communications," *Entropy*, vol. 23, no. 7, p. 880, 2021.

[10] M. Shirvanimoghaddam, H. Khayami, Y. Li, and B. Vucetic, "Dynamic HARQ with guaranteed delay," in *2020 IEEE Wireless Communications and Networking Conference (WCNC)*. IEEE, 2020, pp. 1–6.

[11] B. Makki, T. Svensson, G. Caire, and M. Zorzi, "Fast HARQ over finite blocklength codes: A technique for low-latency reliable communication," *IEEE Transactions on Wireless Communications*, vol. 18, no. 1, pp. 194–209, 2019.

[12] C. Sahin, L. Liu, E. Perrins, and L. Ma, "Delay-sensitive communications over ir-harq: Modulation, coding latency, and reliability," *IEEE Journal on Selected Areas in Communications*, vol. 37, no. 4, pp. 749–764, 2019.

[13] Y. Polyanskiy, H. V. Poor, and S. Verdú, "Channel coding rate in the finite blocklength regime," *IEEE Transactions on Information Theory*, vol. 56, no. 5, p. 2307, 2010.

[14] F. Nadeem, M. Shirvanimoghaddam, Y. Li, and B. Vucetic, "Non-orthogonal HARQ for URLLC: Design and analysis," *IEEE Internet of Things Journal*, pp. 1–1, 2021.

[15] Q. Zhang and S. A. Kassam, "Finite-state Markov model for Rayleigh fading channels," *IEEE Transactions on communications*, vol. 47, no. 11, pp. 1688–1692, 1999.

[16] H. S. Wang and N. Moayeri, "Finite-state Markov channel—a useful model for radio communication channels," *IEEE transactions on vehicular technology*, vol. 44, no. 1, pp. 163–171, 1995.

[17] P. Sadeghi, R. A. Kennedy, P. B. Rapajic, and R. Shams, "Finite-state Markov modeling of fading channels—a survey of principles and applications," *IEEE Signal Processing Magazine*, vol. 25, no. 5, pp. 57–80, 2008.

[18] F. Nadeem, M. Shirvanimoghaddam, Y. Li, and B. Vucetic, "Non-orthogonal HARQ for delay sensitive applications," in *IEEE International Conference on Communications (ICC)*. IEEE, 2020, pp. 1–6.